On the Nature of Blueshifting Hydrogen Bonds

ARTICLE *in* CHEMISTRY - A EUROPEAN JOURNAL · JULY 2014

Impact Factor: 5.73 · DOI: 10.1002/chem.201402189 · Source: PubMed

ChemPubSoc Europe

DOI: 10.1002/chem.201402189

CHEMISTRY
A European Journal
Full Paper

Density Functional Calculations

On the Nature of Blueshifting Hydrogen Bonds

Yirong Mo,*[a] Changwei Wang,[b] Liangyu Guan,[a] Benoît Braïda,[c] Philippe C. Hiberty,[d] and Wei Wu[b]

Abstract: The block-localized wave function (BLW) method can derive the energetic, geometrical, and spectral changes with the deactivation of electron delocalization, and thus provide a unique way to elucidate the origin of improper, blueshifting hydrogen bonds versus proper, redshifting hydrogen bonds. A detailed analysis of the interactions of F_3CH with NH_3 and OH_2 shows that blueshifting is a long-range phenomenon. Since among the various energy components contributing to hydrogen bonds, only the electrostatic interaction has long-range characteristics, we conclude that the contraction and blueshifting of a hydrogen bond is largely caused by electrostatic interactions. On the other hand, lengthening and redshifting is primarily due to the short-range $n(Y)\rightarrow\sigma^*(X-H)$ hyperconjugation. The competition between these two opposing factors determines the final frequency change direction, for example, redshifting in $F_3CH\cdots NH_3$ and blueshifting in $F_3CH\cdots OH_2$. This mechanism works well in the series $F_nCl_{3-n}CH\cdots Y$ ($n=0$–3, $Y=NH_3$, OH_2, SH_2) and other systems. One exception is the complex of water and benzene. We observe the lengthening and redshifting of the O–H bond of water even with the electron transfer between benzene and water completely quenched. A distance-dependent analysis for this system reveals that the long-range electrostatic interaction is again responsible for the initial lengthening and redshifting.

Introduction

Hydrogen-bonding interactions ubiquitously exist in chemical and biological systems and play fundamental roles in the structure, function, and dynamics of chemical and biological systems.[1] Experimentally, the existence of hydrogen bonds can be probed using NMR,[2] IR spectroscopies,[3] and Compton profile anisotropies[4] techniques. Although very often the distances in hydrogen bonds are used as an identification of hydrogen bonds, we note that sometimes the seemingly short distance between X and Y in the X–H···Y construct may result from the structural constraints of the surrounding molecular frame.[5] Generally, the hydrogen bond X–H···Y refers to the particular interaction between an electron-deficient hydrogen atom and an atom (i.e., electronegative atoms such as F, N, or O) or group (e.g., a π-electron cloud) of excessive electrons, which is believed to be predominantly electrostatic in nature,[1e,f,6] although electron transfer from the electron-excessive moiety Y to the electron-deficient H (i.e., hyperconjugation) or partial covalent interactions may also be important.[4,7] Based on the electrostatic model, the X–H bond is lengthened and weakened since the negatively charged Y pulls the positively charged H atom closer to it.[8] Alternatively, the charge-transfer theory suggests the movement of a pair of electrons (mostly a lone pair) on Y to the X–H antibonding orbital, which weakens and consequently elongates the X–H bond and causes its stretching vibrational frequency redshifting with increased intensity.[9] For a long time, the redshift with enhanced intensity in IR spectra has been regarded as a "fingerprint" of hydrogen bonds.[10]

However, there are also "improper, blueshifting" hydrogen bonds in which the X–H bond length contracts, and its stretching mode shifts to higher frequency with reduced intensity (rare cases such as the enflurane···acetone complex with increased intensity have been found recently[11]).[12] The first experimental evidence of a blueshift in the X–H stretching frequency upon the formation of a hydrogen-bonding complex was obtained by Trudeau et al.,[13] who measured an association of fluoroparaffins containing the $-CHF_2$ group with various proton acceptors and found the shift of C–H stretch frequency to higher values. Further proof was provided in 1989 by Buděšínský et al.,[14] who reported the blueshift of chloroform upon complexation with triformylmethane, and in 1997

[a] Prof. Dr. Y. Mo, L. Guan
Department of Chemistry
Western Michigan University, Kalamazoo, MI 49008 (USA)
Fax: (+1) 269-387-2909
E-mail: ymo@wmich.edu

[b] Dr. C. Wang, Prof. Dr. W. Wu
The State Key Laboratory of Physical Chemistry of Solid Surfaces
Fujian Provincial Key Laboratory of Theoretical
and Computational Chemistry
and College of Chemistry and Chemical Engineering
Xiamen University, Xiamen, Fujian 361005 (P.R. China)

[c] Prof. Dr. B. Braïda
Sorbonne Universités
UPMC Univ Paris 06, UMR 7616, LCT, 75005, Paris (France)
CNRS, UMR 7616, LCT, 75005, Paris (France)

[d] Prof. Dr. P. C. Hiberty
Laboratoire de Chimie Physique
UMR CNRS 8000, Université de Paris Sud
91405 Orsay Cédex (France)

by Boldeskul et al.,[15] who measured the IR spectra of haloforms in various proton acceptors. Direct evidence of the blueshift in gas phase was missing until 1999, when a complex between fluorobenzene and chloroform was studied by using double-resonance IR ion-depletion spectroscopy by Hobza and co-workers.[16] The experimental value of the blueshift of the chloroform C–H stretch frequency (14 cm^{-1}) agreed well with the theoretical prediction (12 cm^{-1}). So far, a large variety of improper, blueshifting hydrogen bonds have been confirmed experimentally in the gas or liquid phases and/or identified computationally. This includes C–H···π,[1d,12a,16–17] C–H···O/S,[12c,14–15,18] C–H···F,[19] and S–H···N/P.[20] In most cases, X is a carbon atom. But a carbon center is not a requisite condition, as Si–H···N/O, N–H···F, P–H···O/N, and Cl–H···O/F, and so on, all have blueshifts.[21] Even rare-gas centered improper blueshifting hydrogen bond complexes have been probed theoretically[22] and experimentally.[23]

With the phenomena of blueshifting hydrogen bonds firmly established, an accompanied endeavor is to elucidate their mechanisms and reconcile the new findings with the existing theories for the conventional redshifting hydrogen bonds. By examining the behavior of the hydrogen donor in an electric field, Hobza et al. indicated that the negative sign of the dipole moment derivative with respect to the stretching coordinate is a key for the blueshifting of hydrogen bonds.[18a,24] Noting that blueshifts can be well reproduced at the HF level, Li et al. showed that orbital interactions lengthen the C–H bond in the F_3CH···FH complex at larger distance and thus cannot be the source of the blueshift.[21a] Their analyses suggested that short-range Pauli repulsion between the proton donor and proton acceptor, which balances their electrostatic attraction at the equilibrium geometry of the overall complex, shortens the C–H bond and is the cause for blueshifts. In accord with the view that there are no fundamental distinctions between the classical and improper hydrogen bonds,[18b,24–25] Alabugin and co-workers identified two main competing factors, namely the n(Y)→σ*(X–A) hyperconjugation and the rehybridization and polarization of the X–H bond, based on the natural bond orbital (NBO) analyses.[26] The rehybridization enhances the s character of the hybrid orbital on X,[27] and thus results in the shortening of the X–H bond, whereas the n(Y)→σ*(X–H) hyperconjugation weakens and lengthens the X–H bond. The balance of these two counteracting forces decides whether a hydrogen bond has a redshifted or blueshifted stretching frequency.[26a] However, Joseph and Jemmis argued that there is no obvious relationship between the s character on one atom and the bond length, as the approach of the two water molecules increases the s character at O but continuously lengthens (rather than shortens) the O–H bond even before the hyperconjugation plays its role.[28] Instead, they offered a unified explanation centered on the classical electrostatic interactions. On one hand, the presence of Y polarizes the X–H bond and makes the electronegative X more negatively charged and H more positively charged, and the electrostatic attraction between them consequently shortens the X–H bond; on the other hand, the attraction between H and electron-rich Y leads to the elongation of the X–H bond. The equilibrium geometry and properties of a hydrogen-bonding system come from the competition of these two opposing forces. In improper blueshifting hydrogen bonds, the former dominates, whereas the latter is superior in proper redshifting hydrogen bonds.[28] The polarization of the X–H bond can also be monitored by its bond critical point in the quantum theory of atoms in molecules (QTAIM) analysis.[29]

To precisely probe the role of electron transfer (hyperconjugation) in the hydrogen bonds, here we apply the block-localized wave function (BLW) method,[30] which is a variant of ab initio valence bond (VB) methods,[31] to the study of blueshifting hydrogen bonds. The significance of the BLW lies in its unique definition and optimization of the hypothetical electron-localized Lewis state, in which the hyperconjugation between the hydrogen donor and acceptor is strictly turned off. This is achieved by limiting the expansion of one-electron molecular orbitals.[32] The geometrical and vibrational frequency changes due to the electrostatic and Pauli repulsion interactions but not the electron transfer from other interacting partners, can be used to critically justify the role of hyperconjugation in the red- and blueshifting hydrogen bonds, similar to the previous study of the interaction of carbon monoxide with neutral and positively charged metal centers.[33] In this work, we employ the BLW method to analyze a series of red- and blueshifting hydrogen-bonding complexes, in attempt to elucidate their origins from a new perspective with a set of uniform concepts.

Results and Discussion

Comparison of a set of similar systems exhibiting different frequency changes

It has been a consensus that there is no fundamental difference between red- and blueshifting hydrogen-bonding systems, both of which result from the balance of the same competing forces at the equilibrium structures. A notable question, however, is whether the blueshifting is related to the electron transfer between the hydrogen bond donor (X–H) and acceptor (Y), no matter what the extent is. Based on NBO analyses, Hobza and co-workers[12c,18d,34] found that there is considerable electron transfer from Y to orbitals of other atoms bonded to X rather than directly to the anti-bond orbital of the X–H bond. This kind of remote electron transfer rearranges the molecular geometry and leads to the contraction of the X–H bond. However, most of the explanations are based on the Pauli repulsion (together with hyperconjugation or orbital mixing),[12a,21a] electric field,[10b,18a,24] rehybridization,[26a] and electrostatic interaction[28] and thus are not related to the electron transfer from the hydrogen bond acceptor to the hydrogen bond donor. Yet, so far there are few ways to derive the frequencies in the hypothetical cases without any such kind of electron transfers.

Here we use the BLW method to examine a set of systems including three pairs of comparable systems with different behaviors in frequency variations. The first pair consists of ionic complexes H_3CH···Cl^- (**1**) and $BrCH_3$···Cl^- (**2**), the second pair in-

Table 1. Variation of X–H bond length (ΔR in [Å]), stretching vibration frequency ($\Delta\nu$ in [cm^{-1}]) and IR intensity (ΔI in [$Debye^2/m_uÅ^{-2}$]) from monomers to complexes computed at the M05-2X/6-311+G(d,p) level of theory.[a]

System	Regular DFT			BLW-DFT		
	ΔR	$\Delta\nu$	ΔI	ΔR	$\Delta\nu$	ΔI
$H_3CH\cdots Cl^-$ (**1**)	0.0036	−41.4	1.206	0.0007	5.80	−0.040
$BrCH_3\cdots Cl^-$ (**2**)	−0.0039	58.2	−0.089	−0.0030	45.1	−0.081
$HOH\cdots C_6H_6$ (**3**)	0.0032	−50.7	1.352	0.0017	−20.1	0.509
$F_3CH\cdots C_6H_6$ (**4**)	−0.0029	44.9	−0.613	−0.0030	59.7	−0.376
$F_3CH\cdots NH_3$ (**5**)	0.0006	−12.3	0.244	−0.0023	35.5	0.639
$F_3CH\cdots OH_2$ (**6**)	−0.0017	30.0	−0.544	−0.0026	45.0	−0.544

[a] These data result from the differences between complexes and monomers, that is, $\Delta R = R$(complex) − R(monomer) and $\Delta\nu = \nu$(complex) − ν(monomer).

cludes HOH···benzene (**3**) and $F_3CH\cdots$benzene (**4**), and the third pair involves $F_3CH\cdots NH_3$ (**5**) and $F_3CH\cdots OH_2$ (**6**). We first performed regular DFT calculations and Table 1 summarizes the major changes from monomers to complexes. Results show that **1**, **3**, and **5** are proper, redshifting hydrogen-bonding systems, whereas **2**, **4**, and **6** are improper, blueshifting hydrogen-bonding systems. The redshifting is associated with the lengthening of hydrogen bonds and accompanied with the increasing of intensities. In contrast, the blueshifting is linked with the shortened hydrogen bonds and reduced vibrational intensities.

Interestingly, the BLW optimizations at the same theoretical level with the same basis set show that the shutdown of electron transfers between a hydrogen bond donor and an acceptor has a much bigger impact on reshifting systems than blueshifting systems. For **1**, **3**, and **5**, the hydrogen bond stretching frequencies increases by 46.2, 30.6, and 47.8 cm^{-1}, respectively, with the deactivation of the electron-transfer interaction. But for **2**, **4**, and **6**, the changes are −13.1, 14.8, and 15.0 cm^{-1}. As a consequence, if the electron transfer were turned off, all hydrogen bonds except **3** would be blueshifted. In addition, the good correlation between bond lengths and frequencies is partially lost, as in **1** we still observe a trivial bond lengthening, though it is now a weakly blueshifting system. Among the six systems studied here, compound **3** is exceptional because the O–H bond lengthens and redshifts its stretching frequency with the approach of the benzene ring, even when the electron transfer from the π cloud of benzene to σ^*(O–H) is completely disabled. Detailed analysis of this case will be presented in a following subsection.

To directly view the electron density redistribution due to the approaching of interacting partners, we plot the electron density difference (EDD) maps. At the optimal geometry of a complex, the EDD between the BLW and the sum of individual monomers reflects the polarization of the electron density within each monomer, whereas the difference between the regular DFT and BLW highlights the electron transfer between the two monomers. Figure 1shows the EDD maps of the three pairs due to the polarization effect, in which the light color represents a loss and the darker refers to a gain of electron density. For the first pair, the negatively charged chloride is attracted by and subsequently polarized toward the positively charged hydrogen atom. In contrast, the electron density around the hydrogen atom(s) is pushed back. In **1**, in which the hydrogen bond donor is methane, the three other hydrogen atoms gain the electron density and the electron density in the middle of C–H bond seems enhanced. This electron density enhancement could lead to the strengthening and the subsequent blueshifting stretching frequency (5.8 cm^{-1}) of the hydrogen bond, despite the slight bond lengthening (0.0007 Å). Similarly, in **2**, the electron density on the three hydrogen atoms is shifted to both carbon and bromine, or more precisely to σ^*(Br–C) as Figure 1 shows. This will result in the lengthening of the Br–C bond. Indeed, our BLW optimization leads to the bond length 1.983 Å in the complex **2**, compared with 1.951 Å in bromomethane. But the C–H bonds are shortened notably (from 1.084 in bromomethane to 1.081 in **2** by 0.003 Å). A similar polarization mode can be observed in the second and third pairs. For all systems **1**–**6**, there seems to be an electron density accumulation in the hydrogen bond X–H with the approach of the hydrogen bond acceptor Y, and this polarization effect is echoed by the blueshifting of the hydrogen bond vibrational frequencies, but with a noticeable exception **3**, which redshifts the frequency by 20.1 cm^{-1} with the lengthening of the hydrogen bond by 0.0017 Å. A probable explanation is the electrostatic repulsion between the π cloud of benzene and the oxygen atom of water molecule, which stretches and weakens the O–H bond.

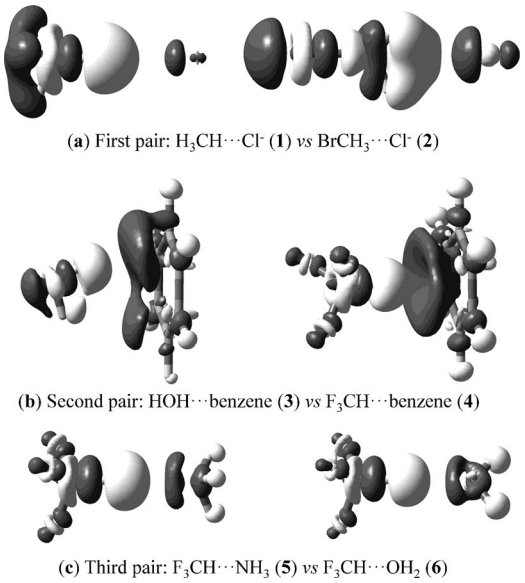

Figure 1. Electron density difference (EDD) maps showing the polarization of the electron density in hydrogen-bonding complexes with reference to their free monomers. Isodensity values: a) and c) 0.001 a.u.; b) 0.0005 a.u.

Figure 2 illustrates the impact of electron transfer from the hydrogen bond acceptor to the donor. For **1**, the chloride anion loses electron density along hydrogen bond direction, and hydrogen atoms are the prime gainer. However, all of the shifted electron density stays between H and Cl^-, and is largely responsible for the covalency of the hydrogen bond.[7b] The electron density on the C–H bond nevertheless decreases. In

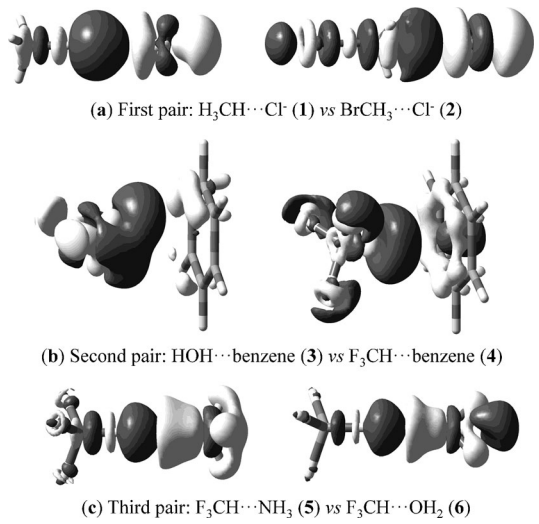

Figure 2. Electron density difference (EDD) maps showing the electron transfer between the hydrogen bond acceptors and donors. Isodensity values are 0.0001 a.u., except for **2** whose value is 0.0002 a.u.

other words, the C–H bond is weakened due to the electron transfer. This is in accord with the general hyperconjugation theory.[22a,26a] Conversely, in **2**, the electron density around Br is enhanced. This kind of relatively remote electron transfer has been identified by Hobza and co-workers.[12c,18d,34] But our results indicate that the blueshifting hydrogen bond in **2** is dominantly caused by other effect than the hyperconjugation, as in the strictly electron-localized state (BLW) the C–H bond already blueshifts its vibrational frequency by 45.1 cm^{-1}, and the electron-transfer effect has a minor impact as it changes the magnitude of the blueshift by only 13.1 to 58.2 cm^{-1}. It should be reminded that in the BLW electron-localized state, apart from the polarization effect, there are also electrostatic and Pauli exchange interactions between $BrCH_3$ and Cl^-. Similar patterns apply to the second pair as well. For **3**, the π electron density of benzene is transferred to the region between OH_2 and the benzene frame, and the electron density around the oxygen of OH_2 is also shifted to the hydrogen bond. As a consequence, the O–H bond is weakened and redshifts its vibrational frequency. In contrast, in **4** there is remote electron transfer (or induced polarization), which makes the electron density around the F atoms of F_3CH increase, and the electron transfer from benzene to F_3CH only moderately weakens the C–H bond and is not enough to reverse its blueshifting of its stretching frequency.

The comparison of the third pair, including $F_3CH\cdots NH_3$ (**5**) and $F_3CH\cdots OH_2$ (**6**), may be the most illuminating, as they are simple yet with dramatic differences. Starting from the separated monomers, BLW computations show that the electron density of F_3CH polarizes quite similarly in both complexes and there is enhancement of electron density in the C–H bond (Figure 1c). The interaction with the hydrogen bond acceptors NH_3 and OH_2 induces blueshifts of comparable magnitude for the C–H bond in HCF_3, by 35.5 and 45.0 cm^{-1}, respectively (Table 1). However, as nitrogen is less electronegative than oxygen, ammonia is more basic than water, and Figure 2c shows that NH_3 loses more electron density than OH_2 to HCF_3. Although most of the transferred density stays in the hydrogen-bonding area as in all other cases **1**–**4**, there are little changes around the fluorine atoms in both systems. Still, some of the transferred density moves to the C–H bond that can be regarded as the $n(Y)\rightarrow\sigma^*(C–H)$ hyperconjugation. Evidently, the density change is more pronounced in **5** than in **6**. As such, although the electron transfer tends to weaken the C–H bond and redshift its frequency, in **5** this weakening force is stronger than the polarization effect, leading to the final redshifting of the hydrogen bond. In contrast, in **6** the electron-transfer effect does not overcompensate the polarization effect, leading to the blueshifting phenomenon.

Influence of the basicity of the hydrogen bond acceptor on the hydrogen bond frequency

The above discussion based on the electron density redistribution is qualitative; more quantitative and detailed analysis of the correlation between frequency shift and hydrogen bond length is thus highly desirable. Here we focus on the third pair, including $F_3CH\cdots NH_3$ and $F_3CH\cdots OH_2$, as they are neutral with well-defined hydrogen bonds. With the same hydrogen bond donor F_3CH, different acceptors like NH_3 and OH_2 exhibit different frequency shifting directions due to their different basicity. To further complete this series and confirm the possible correlation with the basicity of hydrogen bond acceptors, we chose HF, which is a weaker electron donor than H_2O, and explored its interaction with F_3CH along the potential energy surface. The H···Y distance was chosen as the reaction coordinate. Figure 3a1 plots the variations of the C–H distance along the reaction coordinate. Two outstanding features can be observed from this Figure: One is that the shortening of the C–H bond occurs when FH is even far away, that is, the shortening is a long-range phenomenon. We note that Li et al. found that the C–H bond length increases at large distances and goes through a maximum before starting to shorten with different systems (F_2N–H and FO–H) and different constraints (i.e., the X···Y distance as the reaction coordinate).[21a] The other feature is the overlapping of the DFT and BLW curves until at around the DFT equilibrium distance ($R_{H\cdots F}=2.165$ Å). After this point, we observe the disparity of the two curves, and the DFT curves goes up faster than the BLW curve, which further moves down a little before moving up. Since the only difference between the regular DFT and BLW lies in the deactivation of the hyperconjugation between the hydrogen bond donor and acceptor in the latter, the disparity between the DFT and BLW curves reflects the impact of the electron transfer on the geometrical changes. The almost overlapping of the curves at $R_{H\cdots F}>2.25$ Å, thus strongly indicates that the hyperconjugation from the acceptor to the donor is negligible and not responsible for the shortening and blueshifting of the C–H bond in $F_3CH\cdots FH$.

To gain further insight into the hydrogen-bonding interaction and its correlation with the frequency changes, we employed the BLW method to perform energy decomposition analyses[35a,39] for the whole DFT energy profile as shown in Figure 3b1 with numerical values at the optimal geometry listed

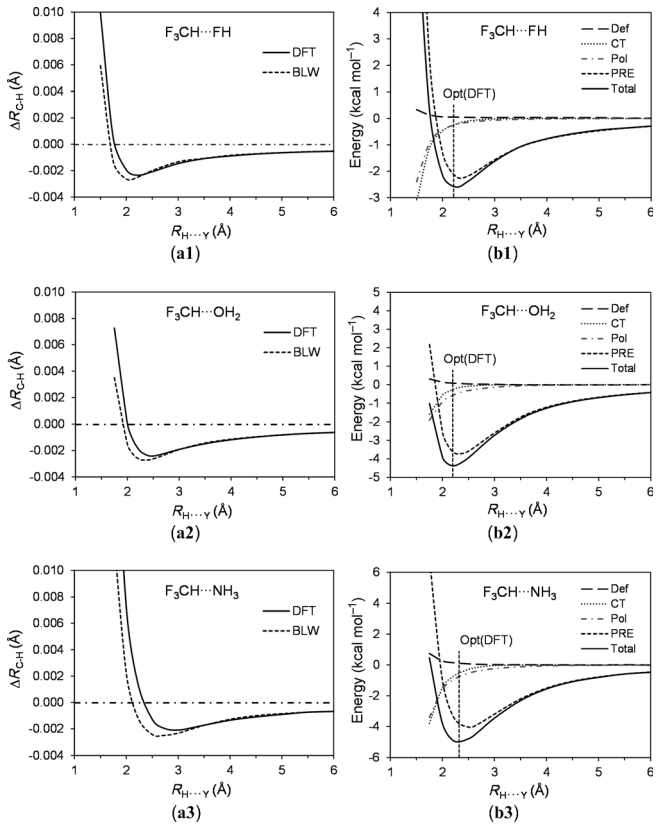

Figure 3. a) Variation of the C–H distance with the distance between H and Y (Y = F, O, and N). b) Variation of energy contributions to the hydrogen-bonding interaction with the hydrogen bond length.

in Table 2. Figure 3 b1 demonstrates that both polarization and charge-transfer energies are short-range and insignificant when $R_{H\cdots F}$ is larger than 2.5 Å. Only when the two interacting partners are in close contact ($R_{H\cdots F} < 2.0$ Å) do these energies decrease dramatically and stabilize the complex. However, these stabilizing energy components are still uncompetitive with the Pauli repulsion and electrostatic energy (PRE),[21a,28] which plays the major role in stabilizing the complex. But when the interacting partners get close enough, the PRE energy increases steeply and overshadows the stabilizing polarization and charge-transfer interactions, and ultimately destabilizes the complex. Clearly, the comparison of Figure 3 a1 and 3 b1 proves that the PRE interaction dominates the shortening and blueshifting of the C–H bond in the $F_3CH\cdots FH$ complex. We note that the key difference between the electrostatic and Pauli exchange interactions composing the PRE energy, is that the former is long-range and the latter is essentially short-range particularly between closed shell molecules,[35] though there is a need for the fine long-range exchange correction within DFT.[36] The study of water dimer has clearly demonstrated that the Pauli exchange is negligible when the H···O distance is larger than 2.5 Å.[35]Thus, we can safely say that in the case of $F_3CH\cdots FH$, the C–H bond shortening and the blueshifting of the stretching vibrational frequency are caused by the electrostatic attraction between F_3CH and FH, in accord with the explanation proposed by Joseph and Jemmis.[28]

Table 2. Intermolecular interaction energy decomposition analyses[a] (ΔE in [kcal mol^{-1}]) for $F_3CH\cdots Y$ (Y = NH_3, OH_2, FH) at their equilibrium geometries and the variations of the X–H bond length (ΔR_{X-H} in [Å]) and stretching vibration frequency ($\Delta\nu$ in [cm^{-1}]) with IR intensity change (ΔI in [Debye^2/m$_u$Å^{-2}]) at the M05-2X/6-311+G(d,p) level of theory.

	ΔE_{Def}	ΔE_{PRE}	ΔE_{pol}	ΔE_{CT}	ΔE_B	ΔR_{X-H}	$\Delta\nu$	ΔI
$F_3CH\cdots FH$	0.04	−2.14	−0.25	−0.24	−2.59	−0.0023	39.9	−0.595
$F_3CH\cdots OH_2$	0.08	−3.53	−0.63	−0.30	−4.38	−0.0017	30.0	−0.544
$F_3CH\cdots NH_3$	0.14	−3.70	−0.83	−0.60	−4.99	0.0006	−12.3	0.244

[a] Hydrogen-bonding energy $\Delta E_B = E(F_3CH\cdots Y) - E(F_3CH) - E(Y) + BSSE = \Delta E_{Def} + \Delta E_{HL} + \Delta E_{pol} + \Delta E_{CT}$ at the optimal geometry of the complex.

We return to the cases of $F_3CH\cdots NH_3$ and $F_3CH\cdots OH_2$ with similar detailed analyses. Much like $F_3CH\cdots FH$, both systems exhibit shortened C–H bond and overlapping DFT and BLW curves at long distances (Figure 3 a2 and 3 a3). Significantly, the disparity of the DFT and BLW curves occurs at 3.15 Å for $F_3CH\cdots NH_3$, at the shorter 2.75 Å distance for $F_3CH\cdots OH_2$, and at the even shorter 2.25 Å distance for $F_3CH\cdots FH$. In other words, the electron-transfer (hyperconjugation) interaction appears at longer distance with the increasing basicity of the hydrogen bond acceptor. On the other hand, the DFT optimal hydrogen bond distances ($R_{H\cdots Y}$) are quite close and fluctuate in all three systems, that is, 2.216 Å in $F_3CH\cdots FH$, 2.165 Å in $F_3CH\cdots OH_2$, and 2.276 Å in $F_3CH\cdots NH_3$. It seems that the comparison of maximum shortening distance is more logic as it increases monotonously with the hydrogen bond acceptor becoming more basic. As a consequence, at the equilibrium distance, the C–H bond has already lengthened with the most basic acceptor, ammonia, and ultimately exhibit the redshifts of the vibrational frequency. We note, however, that if there were no electron transfer, the C–H bond in $F_3CH\cdots NH_3$ would still be shortened with a blueshifting frequency (see the dashed line in Figure 3 a3).

Further energy decomposition analyses (Figure 3 b2 and 3 b3) confirm the short-range characteristics of both polarization and electron-transfer interactions, and the dominating role of the PRE energy component in overall energy curves. Notably, data in Table 2 endorse the conventional view that hydrogen bonding is predominantly electrostatic in nature. Although it accounts for only 7–12% of the total binding energy, the electron-transfer energy increases from the weakest base FH (−0.24 kcal mol^{-1}) to the strongest base NH_3 (−0.60 kcal mol^{-1}). In other words, the greater the hydrogen bond acceptor basicity, the larger the electron donation to the hydrogen bond donor to achieve higher stability. The increasing electron transfer weakens and lengthens the X–H bond, leading to the redshifting of the vibrational frequency. Comparison of Figure 3 b1–3 b3 also shows that the separation between the total energy curve and the PRE energy grows from the least basic HF to the most basic NH_3, indicating the increasing electron-transfer stabilization. Although the hydrogen-bonding interaction is dominated by the electrostatic attraction, the electron-transfer interaction is crucial as it determines the covalency and directionality of the hydrogen bond.

The "abnormal" behavior of the complex of benzene with water

With the disabling of the hyperconjugative interaction, the hydrogen-bonding complexes studied so far, with the exception of the HOH···benzene system, exhibit blueshifting frequencies, and we showed above that the long-range electrostatic interaction is the primary culprit. To explore whether the same force causes the lengthening and redshifting of the O–H bond in the complex of benzene and water, we studied the distance-dependent changes of the energy and geometry. We started from the optimal geometry of benzene and made one O–H bond of water approach perpendicularly to the benzene ring above its center (see the inset in Figure 4a). The distance between the hydrogen atom and the center of the benzene ring is chosen as the reaction coordinate, and at each point the geometrical parameters of the water molecule are fully optimized. Figure 4 shows the variation of the O–H bond length obtained with the regular DFT and BLW methods.

Dramatically different from Figure 3, which shows the shortening of the C–H bond, here we observe the gradual elongation of the O–H bond when the water molecule approaches benzene. At long distances (R > 3 Å), DFT and BLW optimizations result in the same bond lengths. Only when the water is close enough to the benzene ring (R < 3 Å), BLW optimization leads to a shorter O–H distance than the DFT optimization, suggesting the impact of the $\pi \rightarrow \sigma^*$(OH) hyperconjugative interaction. At the BLW optimal geometry ($R_{H\cdots Y} = 2.507$ Å), the O–H bond still stretches by 0.0019 Å and thus its vibrational frequency redshifts. The hyperconjugation shortens the distance between water and benzene ($R_{H\cdots Y} = 2.365$ Å), but the O–H bond length further increases, in accord with the enhanced redshifting. Similar to Figure 3, the BLW energy decomposition of the binding energy between water and benzene (Figure 4b) shows that both polarization and hyperconjugation are negligible at R > 3 Å. In the long range, only the PRE energy, or, more specifically, the electrostatic attraction between the π electrons of benzene and the positively charged hydrogen of water molecule contributes to the binding energy. We note that even at R = 3 Å, the O–H bond already stretches by 0.0013 Å, which may be due to the electrostatic repulsion between the π electrons of benzene and the negatively charged oxygen atom of water molecule. Putting all cases studied so far together (Table 1), we conclude that the initial electrostatic interaction, which is overall attractive, plays the fundamental role in modulating the hydrogen bond vibrational frequency, as it can either blueshift (in most cases) or redshift (in a few cases) the hydrogen bond. The later hyperconjugative interaction, nevertheless, redshifts the vibrational frequency, thus can either reverse the shifting direction or reduce the magnitude of the blueshifts.

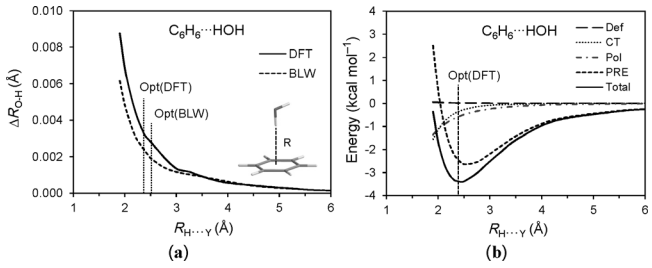

Figure 4. a) Variation of the O–H distance with the distance between H and the center of benzene ring. b) Variation of energy contributions to the hydrogen-bonding interaction with the hydrogen bond length in the C_6H_6···HOH system.

Influence of the acidity of the hydrogen bond donor on the hydrogen bond frequency

So far we have demonstrated that the hyperconjugation from the hydrogen bond acceptor to the donor is the cause for the redshifting of the stretching vibrational frequency, and the blueshifting largely results from the electrostatic interaction between the acceptor and the donor. The competition between these two opposing factors determines the final frequency change direction for each complex compared with the individual hydrogen bond donor. With the same hydrogen bond donor F_3CH, we observe a gradual increase of the hyperconjugation effect with the increasing basicity of the hydrogen bond acceptor from FH to OH_2 to NH_3. Here we expand the scope of the study by examining the frequency changes when using the same hydrogen bond acceptor (Y = NH_3, OH_2 and SH_2) but different hydrogen bond donors. We performed geometry optimizations, frequency computations and energy decomposition analyses at the same M05-2X/6-311 + G(d,p) level of theory. Table 3 summarizes the major results for three groups, each of which corresponding to combination of the different donors $F_nCl_{3-n}CH$ ($n = 3, 2, 1, 0$) with the same acceptor (NH_3 or OH_2 or SH_2). Whereas the acidity of $F_nCl_{3-n}CH$ increases with decreasing n (p*K*a values for fluoroform and chloroform are 28 and 15.5, respectively), SH_2 is a weaker proton acceptor than OH_2, which is itself a weaker proton acceptor than NH_3.

Two significant findings can immediately be garnered from Table 3. First, with the same hydrogen bond acceptor, the binding energy with $F_nCl_{3-n}CH$ increases with the decreasing n, in accord with its slight increasing acidity. Second, when the hyperconjugative interactions are turned off, BLW optimizations result in uniform blueshifting of the hydrogen bond stretching frequency. For Group 1, NH_3 is a good proton acceptor and the lone pair on nitrogen can interact with the anti-bond orbital on C–H. The strong hyperconjugation leads to the final redshifting in all cases. As expected, the magnitude of redshifts increases with the increasing acidity of the hydrogen bond donor from F_3CH to Cl_3CH. Energy decomposition analyses also show that the charge-transfer energy increases in the same order. For the second group, OH_2 is a weaker proton acceptor, and the subsequent hyperconjugative interaction with $F_nCl_{3-n}CH$ is only about half of the value of NH_3. Thus, the hyperconjugation is not strong enough to revise the direction of frequency changes, though the magnitude is reduced.

Table 3. Energy components for the total bonding energies[a] (ΔE in [kcal mol^{-1}]) for $F_nCl_{3-n}CH\cdots Y$ (Y = NH_3, OH_2, SH_2) using block-localized density functional theory in BLW-ED analysis and stretch vibration frequency changes ($\Delta\nu$ in [cm^{-1}]) .

System	ΔE_{Def}	ΔE_{PRE}	ΔE_{pol}	ΔE_{CT}	ΔE_B	$\Delta\nu$ (DFT)	$\Delta\nu$ (BLW)
Group 1							
$F_3CH\cdots NH_3$	0.14	−3.70	−0.83	−0.60	−5.13	−12.3	35.5
$ClF_2CH\cdots NH_3$	0.13	−3.70	−0.97	−0.70	−5.37	−17.7	45.1
$Cl_2FCH\cdots NH_3$	0.12	−3.76	−1.08	−0.80	−5.64	−24.2	43.9
$Cl_3CH\cdots NH_3$	0.05	−3.48	−1.27	−0.97	−5.72	−61.2	29.4
Group 2							
$F_3CH\cdots OH_2$	0.08	−3.53	−0.63	−0.30	−4.46	30.0	45.0
$ClF_2CH\cdots OH_2$	0.07	−3.44	−0.71	−0.33	−4.48	24.2	48.6
$Cl_2FCH\cdots OH_2$	0.05	−3.38	−0.82	−0.37	−4.58	18.6	50.0
$Cl_3CH\cdots OH_2$	0.06	−3.64	−0.82	−0.47	−4.93	18.2	33.9
Group 3							
$F_3CH\cdots SH_2$	0.02	−1.40	−0.23	−0.36	−1.99	8.7	24.4
$ClF_2CH\cdots SH_2$	0.02	−1.50	−0.23	−0.36	−2.10	7.4	20.9
$Cl_2FCH\cdots SH_2$	0.01	−1.46	−0.29	−0.54	−2.29	−0.4	18.5
$Cl_3CH\cdots SH_2$	0.02	−2.06	−0.37	−0.74	−3.17	−8.5	12.0

[a] $\Delta E_B = E(F_nCl_{3-n}CH\cdots Y) - E(F_nCl_{3-n}CH) - E(Y) + BSSE = \Delta E_{Def} + \Delta E_{HL} + \Delta E_{pol} + \Delta E_{CT}$ in which the complex geometry and monomer geometries are optimized individually.

Although SH_2 is a weaker proton acceptor than OH_2, it is a better electron donor than OH_2, as shown by the charge-transfer stabilization energy for the $F_nCl_{3-n}CH\cdots SH_2$ complexes ranging between the values obtained with NH_3 and OH_2 donor groups. In addition, the much lower PRE energy in Group 3 compared with the other two groups is translated to a much lower blueshifting when the electron transfer is completely shut down. The combination of these facts leads to slight blueshifting in $F_3CH\cdots SH_2$ and $ClF_2CH\cdots SH_2$, but redshifting in the more acidic $ClF_2CH\cdots SH_2$ and $Cl_3CH\cdots SH_2$ complexes.

Conclusion

Due to the popularity and important role of hydrogen bonding in chemical and biological systems, extensive experimental and theoretical studies have been conducted so far, and the discovery of improper, blueshifting hydrogen bonds has considerably renewed the research interests in this field. A general belief is that both proper and improper hydrogen bonds are of the same nature, that is, primarily electrostatic. The subtle hyperconjugative interaction from the hydrogen bond acceptor to the donor plays a critical role in the directionality (covalency) of the lengthening and the redshifting of proper hydrogen bonds. An opposing force (which is not obvious and thus secondary in conventional hydrogen bonds) shows up and dominates in improper, blueshifting hydrogen bonds. Proposals for the opposing force ranges from electric fields,[10b] Pauli repulsion,[12a,21a] the rehybridization and polarization of the hydrogen bond,[26a] or simply the classical electrostatic interaction itself.[28] However, it is generally agreed that the equilibrium geometry (hydrogen bond lengthening or shortening) and properties (the red- or blueshifting of the hydrogen bond) of a hydrogen-bonding system result from the competition of the two opposing factors.

In this work, we study the hydrogen bonds by means of the BLW method,[30] which can quantitatively probe the energetic, geometrical, and spectral impact of hyperconjugation on hydrogen-bonding complexes. We first examined three pairs and made one-to-one comparisons for each pair, as one exhibits redshifting, whereas the other exhibits blueshifting in each pair. It is found that, except in the complex of $HOH\cdots C_6H_6$, all hydrogen bonds are blueshifting when the hyperconjugative interactions are deactivated. A subsequent detailed analysis on complexes of $F_3CH\cdots NH_3$ (redshifting system) and $F_3CH\cdots OH_2$ (blueshifting system) revealed that blueshifting is a long-range phenomenon whereas redshifting is a short-range phenomenon. The BLW energy decomposition scheme interprets the binding interaction in terms of deformation, Pauli repulsion and electrostatic (PRE), polarization and charge (electron)-transfer energy components. Among these terms, only the PRE energy has long-range characteristics, so we propose that the PRE interaction is related to the blueshifting of hydrogen bonds. However, as the PRE energy is composed of the electrostatic interaction and Pauli exchange repulsion, and the latter is once again short-range, we conclude that the blueshifting is caused by the classical electrostatic interactions between hydrogen bond donor and acceptor, a view developed by Joseph and Jemmis.[28] But the lengthening and redshifting largely result from the $n(Y)\rightarrow\sigma^*(X{-}H)$ hyperconjugative interaction.[26a] The competition between the electrostatic and hyperconjugative interactions decides the eventual frequency change in any hydrogen-bonding system. This general mechanism is well-endorsed by the analyses of a series of systems $F_nCl_{3-n}CH\cdots Y$ (n = 0–3, Y = NH_3, OH_2, SH_2). In a few cases, such as the benzene–water complex, a stretched and redshifting hydrogen bond is found even when the $\pi\rightarrow\sigma^*(OH)$ hyperconjugative interaction is quenched. Detailed analysis shows again that the long-range electrostatic interaction plays the commanding role.

In summary, electrostatic interactions play a key role in determining the direction of hydrogen bond vibrational frequency shifts, and it is the only long-range interaction among the various energy terms contributing to the formation of hydrogen bonds. In most cases, electrostatic interactions result in the blueshifting of a hydrogen bond, and the subsequent short-range hyperconjugation has an opposite effect. If the latter is stronger than the former, redshifting will be observed, otherwise blueshifting is the consequence. In certain cases, however, the electrostatic interactions favor a redshifting, and the subsequent hyperconjugation only further enhances the magnitude of this redshift.

Computational Methods

Block-localized wave function (BLW) method

According to the VB theory, a molecule can be described with one or a few Lewis structures, and each Lewis structure can be uniquely represented with a Heitler–London–Slater–Pauling (HLSP) function, which can be further expanded into a number of Slater deter-

minants.[31] Unlike popular molecular orbital (MO)-based methods, in which all MOs are delocalized and constrained to be orthogonal, orbitals in VB theory are usually local and nonorthogonal. The localization and nonorthogonality of orbitals make the ab initio VB computations physically and chemically appealing but computationally challenging. One significant way to simplify the computational complexity and reduce the computational cost is to represent a set of covalent bonds with nonorthogonal but doubly occupied fragment-localized orbitals (or group functions[37]).[32,38] We have been developing the BLW method, in which a BLW corresponds to a unique electron-localized diabatic state (usually the most stable resonance state).[30] The fundamental assumption is that the total electrons and primitive basis functions can be divided into several subgroups (blocks), and each MO is expanded in only one block and called block-localized MO (BL-MO). Orbitals in the same subspace are subject to the orthogonality constraint, but orbitals belonging to different subspaces are free to overlap and thus are nonorthogonal. In the present work, the BLW corresponds to a diabatic state in which the electron transfer (hyperconjugation) between the hydrogen bond donor and acceptor is strictly "deactivated". Both the geometrical and energetic changes due to the electron-transfer effect thus can be explored.

Based on the BLW method, we also proposed an energy decomposition Scheme in which the molecular binding energy is decomposed into deformation energy (ΔE_{def}), Pauli repulsion and electrostatic energy (ΔE_{PRE}), polarization energy (ΔE_{pol}) and charge (electron)-transfer energy (ΔE_{CT}) contributions. If needed, an electron correlation energy term can be added.[35a,39] The basis set superposition error (BSSE)[40] is contained in the charge-transfer term.

Computational details

We first made one-to-one comparisons for three similar pairs, each of which is composed of one redshifting and one blueshifting hydrogen-bonding systems, including $H_3CH\cdots Cl^-$ versus $BrCH_3\cdots Cl^-$, HOH···benzene versus F_3CH···benzene, and $F_3CH\cdots NH_3$ versus $F_3CH\cdots OH_2$ at their equilibrium geometries. Detailed analyses of the changes along the potential energy surfaces were subsequently conducted for the same hydrogen bond donor F_3CH with different acceptors (NH_3, OH_2 and FH). Similar analysis was performed for the exceptional case of benzene with water. Finally, we compare the interactions between different hydrogen bond donors (F_3CH, ClF_2CH, Cl_2FCH, and Cl_3CH) with different acceptors (NH_3, OH_2, and SH_2). Geometry optimizations and calculations for adiabatic states with the regular DFT, and diabatic states with the BLW methods, were performed with our in-house version of the quantum mechanical software GAMESS at the M05–2X/6–311 + G(d,p) level of theory.[41] All of the hydrogen-bonded systems were found to be actual minima as confirmed by frequency calculations. Hydrogen bond energies were corrected for BSSE with the counterpoise method.[40]

Acknowledgements

This work was supported by the US National Science Foundation under the grants CHE-1055310 and CNS-1126438. C.W. acknowledges the financial support from the China Scholarship Council (CSC). W.W. is grateful for the funding from the National Science Foundation of China (20873106) and the Ministry of Science and Technology of China (2011CB808504).

Keywords: density functional calculations · electron transfer · hydrogen bonds · hyperconjugation · vibrational spectroscopy

[1] a) G. Gilli, P. Gilli, *The Nature of the Hydrogen Bond: Outline of a Comprehensive Hydrogen Bond Theory*, Vol. 23, Oxford University Press, New York (USA), **2009**; b) S. J. Grabowski, in *Challenges and Advances in Computational Chemistry and Physics*, Vol. 3 (Ed.: J. Leszczynski), Springer, Dordrecht, The Netherlands, **2006**; c) Y. Marechal, *The Hydrogen Bond and the Water Molecule: The Physics and Chemistry of Water*, Aqueous and Bio-Media, Elsevier Science, Amsterdam, **2007**; d) M. Nishio, M. Hirota, Y. Umezawa, *The CH/Interaction. Evidence, Nature and Consequences*, Wiley-VCH, New York, **1998**; e) G. R. Desiraju, T. Steiner, *The Weak Hydrogen Bond: In Structural Chemistry and Biology (International Union of Crystallography Monographs on Crystallography)*, Oxford University Press, Oxford (USA), **2001**; f) G. A. Jeffrey, *An Introduction to Hydrogen Bonding*, Oxford University Press, Oxford (USA), **1997**; g) S. Scheiner, *Hydrogen Bonding: A Theoretical Perspective, Oxford University Press*, Oxford (USA), **1997**; h) C. B. Aakeröy, A. M. Beatty, K. R. Lorimer, *Struct. Chem.* **1999**, *10*, 229–242; i) W. W. Cleland, M. M. Kreevoy, *Science* **1994**, *264*, 1887–1890; j) P. A. Frey, S. A. Whitt, J. B. Tobin, *Science* **1994**, *264*, 1927–1930; k) A. J. Lough, S. Park, R. Ramachandran, R. H. Morris, *J. Am. Chem. Soc.* **1994**, *116*, 8356–8357; l) E. Peris, J. C. Lee, J. R. Rambo, O. Eisenstein, R. H. Crabtree, *J. Am. Chem. Soc.* **1995**, *117*, 3485–3491; m) G. Gilli, F. Bellucci, V. Ferretti, V. Bertolasi, *J. Am. Chem. Soc.* **1989**, *111*, 1023–1028; n) V. Bertolasi, P. Gilli, V. Ferretti, G. Gilli, *J. Am. Chem. Soc.* **1991**, *113*, 4917–4925; o) G. R. Desiraju, *Acc. Chem. Res.* **2002**, *35*, 565–573.

[2] T. Tuttle, J. Graefenstein, A. Wu, E. Kraka, D. Cremer, *J. Phys. Chem. B* **2004**, *108*, 1115–1129.

[3] B. Brauer, R. B. Gerber, M. Kabelac, P. Hobza, J. M. Bakker, A. G. A. Riziq, M. S. de Vries, *J. Phys. Chem. A* **2005**, *109*, 6974–6984.

[4] E. D. Isaacs, A. Shukla, P. M. Platzman, D. R. Hamann, B. Barbiellini, C. A. Tulk, *Phys. Rev. Lett.* **1999**, *82*, 600–603.

[5] a) P. Sanz, O. Mó, M. Yáñez, J. Elguero, *J. Phys. Chem. A* **2007**, *111*, 3585–3591; b) J. F. Beck, Y. Mo, *J. Comput. Chem.* **2007**, *28*, 455–466; c) C. L. Perrin, *Acc. Chem. Res.* **2010**, *43*, 1550–1557.

[6] a) L. C. Pauling, *The Nature of the Chemical Bond*, 3rd Ed., Cornell University Press, Ithaca, NY, **1960**; b) K. Morokuma, *Acc. Chem. Res.* **1977**, *10*, 294–300.

[7] a) K. G. Tapan, N. S. Viktor, R. K. Patrick, R. D. Ernest, *J. Am. Chem. Soc.* **2000**, *122*, 1210–1214; b) S. J. Grabowski, *Chem. Rev.* **2011**, *111*, 2597–2625; c) M. S. Gordon, J. H. Jensen, *Acc. Chem. Res.* **1996**, *29*, 536–543; d) S. Y. Liu, C. E. Dykstra, *J. Phys. Chem.* **1986**, *90*, 3097–3103; e) P. A. Kollman, L. C. Allen, *Chem. Rev.* **1972**, *72*, 283–303; f) C. F. Guerra, F. M. Bickelhaupt, E. J. Baerends, *ChemPhysChem* **2004**, *5*, 481–487.

[8] R. F. W. Bader, *Can. J. Chem.* **1964**, *42*, 1822–1834.

[9] a) H. Ratajczak, *J. Phys. Chem.* **1972**, *76*, 3000–3004; b) W. H. Thompson, J. T. Hynes, *J. Am. Chem. Soc.* **2000**, *122*, 6278–6286.

[10] a) A. Allerhand, P. v. R. Schleyer, *J. Am. Chem. Soc.* **1963**, *85*, 1715–1725; b) W. Zierkiewicz, P. Jurečka, P. Hobza, *ChemPhysChem* **2005**, *6*, 609–617.

[11] a) W. Zierkiewicz, B. Czarnik-Matusewicz, D. Michalska, *J. Phys. Chem. A* **2011**, *115*, 11362–11368; b) W. Zierkiewicz, R. Zalesny, P. Hobza, *Phys. Chem. Chem. Phys.* **2013**, *15*, 6001–6007.

[12] a) P. Hobza, V. Špirko, H. L. Selzle, E. W. Schlag, *J. Phys. Chem. A* **1998**, *102*, 2501–2504; b) P. Hobza, Z. Havlas, *Chem. Rev.* **2000**, *100*, 4253–4264; c) B. J. van der Veken, W. A. Herrebout, R. Szostak, D. N. Shchepkin, Z. Havlas, P. Hobza, *J. Am. Chem. Soc.* **2001**, *123*, 12290–12293; d) M. Egli, S. Sarkhel, *Acc. Chem. Res.* **2007**, *40*, 197–205; e) A. M. Wright, A. A. Howard, C. Howard, G. S. Tschumper, N. I. Hammer, *J. Phys. Chem. A* **2013**, *117*, 5435–5446.

[13] G. T. Trudeau, J. M. Dumas, P. Dupuis, M. Guerin, C. Sandorfy, *Top. Curr. Chem.* **1980**, *93*, 91–125.

[14] M. Buděšínský, P. Fiedler, Z. Arnold, *Synthesis* **1989**, *1989*, 858–860.

[15] I. E. Boldeskul, I. F. Tsymbal, E. V. Ryltsev, Z. Latajka, A. J. Barnes, *J. Mol. Struct.* **1997**, *436–437*, 167–171.

[16] P. Hobza, V. Špirko, Z. Havlas, K. Buchhold, B. Reimann, H. D. Barth, B. Brutschy, *Chem. Phys. Lett.* **1999**, *299*, 180–186.

[17] B. Reimann, K. Buchhold, S. Vaupel, B. Brutschy, Z. Havlas, V. Spirko, P. Hobza, *J. Phys. Chem. A* **2001**, *105*, 5560 – 5566.
[18] a) P. Hobza, Z. Havlas, *Chem. Phys. Lett.* **1999**, *303*, 447 – 452; b) Y. Gu, T. Kar, S. Scheiner, *J. Am. Chem. Soc.* **1999**, *121*, 9411 – 9422; c) N. Karger, A. M. Amorim da Costa, P. J. A. Ribeiro-Claro, *J. Phys. Chem. A* **1999**, *103*, 8672 – 8677; d) W. Zierkiewicz, D. Michalska, Z. Havlas, P. Hobza, *ChemPhysChem* **2002**, *3*, 511 – 518; e) S. N. Delanoye, W. A. Herrebout, B. J. van der Veken, *J. Am. Chem. Soc.* **2002**, *124*, 11854 – 11855.
[19] W. Caminati, S. Melandri, P. Moreschini, P. G. Favero, *Angew. Chem.* **1999**, *111*, 3105 – 3107; *Angew. Chem. Int. Ed.* **1999**, *38*, 2924 – 2925.
[20] M. Solimannejad, M. Gharabaghi, S. Scheiner, *J. Chem. Phys.* **2011**, *134*, 024312.
[21] a) X. S. Li, L. Liu, H. B. Schlegel, *J. Am. Chem. Soc.* **2002**, *124*, 9639 – 9647; b) J. M. Fan, L. Liu, Q. X. Guo, *Chem. Phys. Lett.* **2002**, *365*, 464 – 472; c) S. A. C. McDowell, A. D. Buckingham, *J. Am. Chem. Soc.* **2005**, *127*, 15515 – 15520; d) R. Szostak, *Chem. Phys. Lett.* **2011**, *516*, 166 – 170; e) B. Raghavendra, E. Arunan, *J. Phys. Chem. A* **2007**, *111*, 9699 – 9706.
[22] a) I. V. Alabugin, M. Manoharan, F. A. Weinhold, *J. Phys. Chem. A* **2004**, *108*, 4720 – 4730; b) A. Lignell, L. Khriachtchev, M. Pettersson, M. Räsänen, *J. Chem. Phys.* **2002**, *117*, 961 – 964; c) S. A. C. McDowell, *J. Chem. Phys.* **2003**, *118*, 7283 – 7287; d) S. A. C. McDowell, A. D. Buckingham, *Spectrochim. Acta Part A* **2005**, *61*, 1603 – 1609; e) S. A. C. McDowell, *Mol. Phys.* **2005**, *103*, 2763 – 2768; f) M. V. Sigalov, E. P. Doronina, V. F. Sidorkin, *J. Phys. Chem. A* **2012**, *116*, 7718 – 7725.
[23] A. Lignell, J. Lundell, L. Khriachtchev, M. Räsänen, *J. Phys. Chem. A* **2008**, *112*, 5486 – 5494.
[24] a) K. Hermansson, *J. Phys. Chem. A* **2002**, *106*, 4695 – 4702; b) A. Masunov, J. J. Dannenberg, R. H. Contreras, *J. Phys. Chem. A* **2001**, *105*, 4737 – 4740.
[25] a) S. Scheiner, T. Kar, *J. Phys. Chem. A* **2002**, *106*, 1784 – 1789; b) C. E. Dykstra, *Acc. Chem. Res.* **1988**, *21*, 355 – 361; c) W. L. Qian, S. Krimm, *J. Phys. Chem. A* **2002**, *106*, 6628 – 6636; d) W. L. Qian, S. Krimm, *J. Phys. Chem. A* **2005**, *109*, 5608 – 5618; e) E. Cubero, M. Orozco, P. Hobza, F. J. Luque, *J. Phys. Chem. A* **1999**, *103*, 6394 – 6401.
[26] a) I. V. Alabugin, M. Manoharan, S. Peabody, F. Weinhold, *J. Am. Chem. Soc.* **2003**, *125*, 5973 – 5987; b) A. E. Reed, L. A. Curtiss, F. Weinhold, *Chem. Rev.* **1988**, *88*, 899 – 926.
[27] H. Bent, *Chem. Rev.* **1961**, *61*, 275 – 311.
[28] J. Joseph, E. D. Jemmis, *J. Am. Chem. Soc.* **2007**, *129*, 4620 – 4632.
[29] S. J. Grabowski, *J. Phys. Chem. A* **2011**, *115*, 12789 – 12799.
[30] a) Y. Mo, *J. Chem. Phys.* **2003**, *119*, 1300 – 1306; b) Y. Mo, S. D. Peyerimhoff, *J. Chem. Phys.* **1998**, *109*, 1687 – 1697; c) Y. Mo, L. Song, Y. Lin, *J. Phys. Chem. A* **2007**, *111*, 8291 – 8301.
[31] a) *Valence Bond Theory* (Ed.: D. L. Cooper), Elsevier, Amsterdam, **2002**; b) G. A. Gallup, *Valence Bond Methods: Theory and Applications*, Cambridge University Press, New York, **2002**; c) S. S. Shaik, P. C. Hiberty, *A Chemist's Guide to Valence Bond Theory*, Wiley, Hoboken, New Jersey, **2008**; d) W. Wu, P. Su, S. Shaik, P. C. Hiberty, *Chem. Rev.* **2011**, *111*, 7557 – 7593.
[32] a) H. Stoll, H. Preuss, *Theor. Chim. Acta* **1977**, *46*, 11 – 21; b) H. Stoll, G. Wagenblast, H. Preuss, *Theor. Chim. Acta* **1980**, *57*, 169 – 178; c) E. L. Mehler, *J. Chem. Phys.* **1977**, *67*, 2728 – 2739; d) E. L. Mehler, *J. Chem. Phys.* **1981**, *74*, 6298 – 6306; e) E. Gianinetti, M. Raimondi, E. Tornaghi, *Int. J. Quantum Chem.* **1996**, *60*, 157 – 166; f) A. Famulari, E. Gianinetti, M. Raimondi, M. Sironi, *Int. J. Quantum Chem.* **1998**, *69*, 151 – 158; g) R. Z. Khaliullin, E. A. Cobar, R. C. Lochan, A. T. Bell, M. Head-Gordon, *J. Phys. Chem. A* **2007**, *111*, 8753 – 8765.
[33] K. Nakashima, X. Zhang, M. Xiang, Y. Lin, M. Lin, Y. Mo, *J. Theor. Chem. Comput.* **2008**, *7*, 639 – 654.
[34] P. Hobza, Z. Havlas, *Theor. Chem. Acc.* **2002**, *108*, 325 – 334.
[35] a) Y. Mo, J. Gao, S. D. Peyerimhoff, *J. Chem. Phys.* **2000**, *112*, 5530 – 5538; b) J. H. Jensen, M. S. Gordon, *Mol. Phys.* **1996**, *89*, 1313 – 1325.
[36] A. Savin, in *Recent Developments and Applications of Modern Density Functional Theory* (Ed.: J. M. Seminario), Elsevier, Amsterdam, **1996**, pp. 327 – 357.
[37] R. McWeeny, *Proc. R. Soc. London Ser. A* **1959**, *253*, 242 – 259.
[38] R. S. Mulliken, R. G. Parr, *J. Chem. Phys.* **1951**, *19*, 1271 – 1278.
[39] Y. Mo, P. Bao, J. Gao, *Phys. Chem. Chem. Phys.* **2011**, *13*, 6760 – 6775.
[40] S. F. Boys, F. Bernardi, *Mol. Phys.* **1970**, *19*, 553 – 566.
[41] M. W. Schmidt, K. K. Baldridge, J. A. Boatz, S. T. Elbert, M. S. Gordon, J. J. Jensen, S. Koseki, N. Matsunaga, K. A. Nguyen, S. Su, T. L. Windus, M. Dupuis, J. A. Montgomery, *J. Comput. Chem.* **1993**, *14*, 1347 – 1363.

Received: February 14, 2014
Published online on ■■ ■■, 2014

FULL PAPER

Density Functional Calculations

Y. Mo, C. Wang, L. Guan, B. Braïda, P. C. Hiberty, W. Wu*

■■ – ■■

On the Nature of Blueshifting Hydrogen Bonds

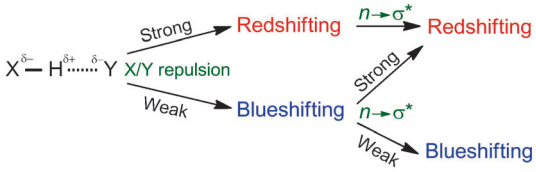

Into the blue (or red)? In most cases, electrostatic interactions result in the blueshifting of a hydrogen bond, whereas the short-range hyperconjugation has an opposite effect (see figure). If the latter is stronger than the former, redshifting will be observed, otherwise blueshifting is the consequence. In certain cases, however, the electrostatic interactions favor redshifting, and the subsequent hyperconjugation only further enhances the magnitude of this redshift.